The Astronomical Journal, 121:453–457, 2001 January

AN ANALYSIS OF THE K I λ7698 LINE PROFILE IN THE HALO TURNOFF STAR HD 84937 AND ITS IMPLICATIONS FOR LITHIUM ISOTOPIC STUDIES

Verne V. Smith
Department of Physics, University of Texas at El Paso, El Paso, TX 79968; and McDonald Observatory, University of Texas at Austin, Austin, TX 78712
Omar Vargas-Ferro
Department of Physics, University of Texas at El Paso, El Paso, TX 79968
David L. Lambert
Department of Astronomy, University of Texas at Austin, Austin, TX 78712
and
John G. Olgin
Department of Physics, University of Texas at El Paso, El Paso, TX 79968
Received 2000 July 18; accepted 2000 September 25

ABSTRACT

The line profile of the resonance line of K I at 7698 Å has been analyzed in the halo turnoff star HD 84937, using a high-resolution ($\lambda/\Delta\lambda = 110{,}000$), high signal-to-noise ratio (S/N = 550) spectrum. Three different groups have reported detecting ^{6}Li in this star, based on a red asymmetry in the Li I λ6707 line profile (^{6}Li displays an isotopic shift of about 0.15 Å to the red, relative to ^{7}Li, in this line). It is possible, however, that convection could introduce this red asymmetry by mass motions of ^{7}Li in the star's atmosphere. At the metallicity of HD 84937, the K I resonance line at 7698 Å is expected to have a similar line strength to the Li I λ6707 feature, and both these lines are resonance transitions. In addition, both potassium and lithium have similar first ionization potentials. The result of these similarities is that the Li I and K I lines are formed at nearly identical regions in the atmosphere of HD 84937. This study presents a line profile analysis of the K I line, which has negligible isotopic splitting and is effectively a single-component line, in HD 84937. Any possible convective motions of sufficient magnitude to produce a spurious detection of ^{6}Li should also produce detectable asymmetries in the K I line. No such asymmetries are found here, strengthening the case that the previously reported detections of ^{6}Li in HD 84937 are real.

Key words: stars: abundances — stars: individual (HD 84937) — stars: Population II

1. INTRODUCTION

The search for the origins of the rare light nuclei of lithium, beryllium, and boron continues, with emphasis now on quantitative comparisons with predictions from theory. The key nucleosynthetic processes for the production of these nuclei are known: (1) the big bang provided some ^{7}Li (as well as H, ^{2}H, ^{3}He, and ^{4}He) but none of the other light nuclides in relevant amounts; (2) spallation interactions between cosmic rays and the interstellar medium provide all of the light nuclides, i.e., ^{6}Li, ^{7}Li, ^{9}Be, ^{10}B, and ^{11}B; (3) $\alpha + \alpha$ fusion reactions between cosmic rays and the ambient gas can produce ^{6}Li and ^{7}Li; (4) neutrino-induced spallation in core-collapse Type II supernovae (SNe II) may produce some ^{7}Li and ^{11}B; and (5) hot bottom burning in asymptotic giant branch (AGB) stars may produce significant quantities of ^{7}Li. In general, gas ejected by stars, except by processes 4 and 5, will be greatly depleted in the light nuclides, because all are astrated through (p, α) reactions at moderate temperatures of, depending on the particular nuclide, $(2\text{–}5) \times 10^6$ K.

With production by these numerous processes, the Galactic chemical evolution of the light elements is a complex story demanding as many and as diverse observational constraints as possible. Isolating the behavior of the two stable lithium isotopes helps in putting together the pieces of the light-element puzzle. Because ^{6}Li is produced only by cosmic-ray interactions (either through spallation or $\alpha + \alpha$ reactions), whereas ^{7}Li not only is produced by these reactions but also has a substantial predicted contribution from the big bang, SNe II, and AGB stars, measurements of the isotopic abundances can, in principle, help to disentangle the various contributions. In addition, ^{6}Li is more easily astrated than ^{7}Li. Probing the ^{6}Li/^{7}Li ratios in stars can therefore provide key data sensitive to stellar mixing processes or mass loss. Observations of the metal-poor, unevolved dwarf and subgiant stars minimizes the impact of galactic chemical evolution effects, with the result that ^{6}Li/^{7}Li ratios in these metal-poor stars provide important constraints on possible astration of ^{7}Li (and the stellar models that predict astration) and therefore on the relation between the observed ^{7}Li abundances and those of the big bang.

Among the metal-poor halo dwarfs and subgiants, ^{6}Li was first detected in the turnoff star HD 84937 ([Fe/H] = −2.2) by Smith, Lambert, & Nissen (1993). Metal-poor stars at and near the main-sequence turnoff are predicted to have retained most or all of their ^{6}Li. This detection was confirmed by Hobbs & Thorburn (1994, 1997) and most recently by Cayrel et al. (1999). In addition, ^{6}Li has also been detected in the halo dwarfs BD +26°3578 (Smith, Lambert, & Nissen 1998), with [Fe/H] = −2.6, and G271-162 (Nissen et al. 2000), with [Fe/H] = −2.2, as well as in two mildly metal-poor halo dwarfs (HD 68284 and HD 130551, with [Fe/H] ∼ −0.6) by Nissen et al. (1999). All of these detections put the ^{6}Li fraction at just a few percent of total Li abundance. The expected source of the ^{6}Li in these old, unevolved stars is thought to be cosmic-ray interactions, although perhaps some measurable amounts

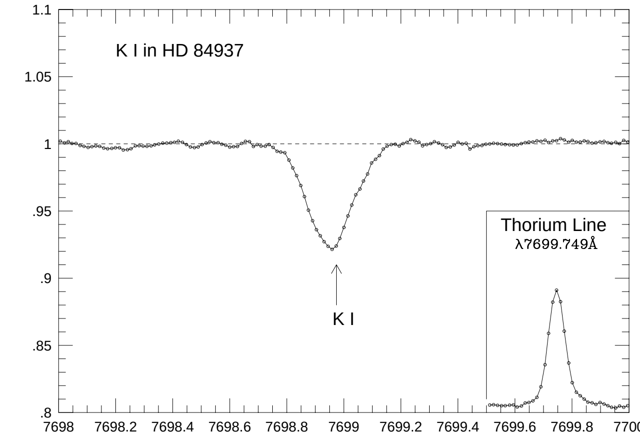

FIG. 1.—Final reduced spectrum of HD 84937 showing the K I 7698.97 Å line. The continuum S/N = 550. A nearby Th II comparison line is shown in the inset: this line effectively defines the instrumental broadening profile.

of ^{6}Li are produced in big bang nucleosynthesis (BBN): Cecil, Yan, & Galovich (1996) have suggested that up to 1% of the total Li produced in BBN might be ^{6}Li. More recent calculations by Vangioni-Flam, Coc, & Cassé (2000) suggest, on the other hand, that the ^{6}Li/^{7}Li ratio from BBN is closer to 10^{-3}, indicating that the small amounts of ^{6}Li in some halo stars (at the few-percent level) are probably of cosmic-ray origin.

These detections of trace amounts of ^{6}Li are based on analysis of high-resolution, high signal-to-noise ratio spectra of the Li I λ6707 resonance doublet. The dominant isotope ^{7}Li provides two lines with a separation of about 0.15 Å, with the red line having a strength half that of the blue line; the small hyperfine splitting is taken into account in the published analyses. The isotopic wavelength shift is such that the stronger ^{6}Li line is almost coincident with the weaker (red) ^{7}Li line, and the weaker ^{6}Li line is shifted an additional 0.15 Å to the red. In short, the ^{6}Li contribution to the 6707 Å stellar line is found by quantifying a small additional red asymmetry of an asymmetric line.

A common concern of observers has been to show that the additional red asymmetry is caused by a trace of ^{6}Li and not by atmospheric effects. For example, convective motions could, in principle, produce a red or blue line asymmetry, depending on whether a line-forming region was dominated by upward- or downward-moving cells and the speed of the convection.

Being the prototype halo star for ^{6}Li studies, HD 84937 is investigated here for possible asymmetric broadening mechanisms (such as convection) that might mimic ^{6}Li. Potassium has nearly the same first ionization potential as lithium (4.34 vs. 5.39 eV, respectively), and at the metallicity of HD 84937, the Li I 6707 Å and K I 7699 Å resonance lines have very similar equivalent widths, i.e., the lines are formed in nearly the same layers of a stellar atmosphere. In previous studies of HD 84937, the various groups have typically used stronger lines, such as the Ca I 6162 Å excited line, to define the intrinsic stellar broadening in the star. However, this stronger line is formed at distinctly higher layers in the star's atmosphere. The differing depths of formation leave open the possibility that differential convection in HD 84937 could produce a red asymmetry in the Li I feature larger than that found for the Ca I lines. The K I 7699 Å line was used by Nissen et al. (2000) in their analysis of the turnoff star G271-162.

2. OBSERVATIONS

High-resolution spectra of HD 84937 were obtained with the cross-dispersed two-dimensional coudé echelle spectrometer on the 2.7 m H. J. Smith reflector at McDonald Observatory (Tull et al. 1995). A Tektronix 2048 × 2048 pixel CCD, with a pixel size of 24 μm, was the detector. The spectrometer plus CCD resulted in a scale of 0.0138 Å pixel^{-1} at 7700 Å. An entrance slit with a projected FWHM of 5 pixels was used, so the effective resolution at the K I line was 0.0690 Å, or $R = \lambda/\Delta\lambda = 111{,}600$. Five separate 1 hr integrations were taken of HD 84937 on the night of 1998 March 16/17, following the star from about $2^{\rm h}.5$ east to $2^{\rm h}.5$ west.

The raw, two-dimensional CCD frames of HD 84937 were reduced to a set of one-dimensional spectra using NOAO's IRAF software packages. Individual program CCD frames had bias frames subtracted from them, with the pixel-to-pixel sensitivity variations removed by dividing by quartz lamp frames. Scattered light in the spectrometer was measured and then subtracted by measuring the light falling in regions between spectral orders (this is the routine APSCATTER in the IRAF package ECHELLE). The defined spectral apertures were used to define the starlight and sum the counts to produce final one-dimensional spectra. These reduced spectra were cleaned of cosmic rays, and thorium-argon reference spectra were used to assign wavelength calibrations (with typical uncertainties of 3–5 mÅ). The individual spectra were combined with the ECHELLE routine SCOMBINE, after the small wavelength shifts caused by the terrestrial diurnal motion and instrumental drift were corrected for.

The final combined spectrum showing the K I line at 7698.97 Å in HD 84937 is shown in Figure 1. The other line from this resonance doublet, λ7664.90, fell off the CCD. The signal-to-noise ratio (S/N) of this spectrum, as defined by the continuum regions outside of the K I absorption, is 550. For comparison, a Th II line is shown in the inset: as mentioned above, the spectrometer entrance slit projects to an FWHM on the CCD of 5 pixels. Using six Th II lines falling in the order containing the K I line, an average FWHM of 4.6 ± 0.2 pixels was measured, corresponding to a measured resolution of 0.0635 Å, or $R = 121{,}200$. Although some small-level fringing occurs in the CCD at the K I wavelength (at a few-percent level), division by the flat field removes this to reasonably high accuracy, and no residual fringing is evident in the spectrum shown in Figure 1.

It is worth comparing the radial velocity for HD 84937 derived from the K I line with those published previously for this star from the Li I line (Smith et al. 1998). The heliocentric radial velocity from Li I is -13.47 ± 0.35 km s^{-1}, while the K I line from this night yields a velocity of -13.94 km s^{-1}. There is, as discussed in previous studies, no evidence that HD 84937 is a binary, insofar as the Li I and K I lines give the same radial velocity (within the uncertainties) as expected for two similar lines formed in the same regions of a single star's atmosphere.

3. ANALYSIS

The Li I 6707 Å line of HD 8493 has been analyzed by a number of investigators (Smith et al. 1993, 1998; Hobbs &

Thorburn 1994, 1997; Cayrel et al. 1999). Techniques similar to those used in the analysis of the Li I feature are adopted and applied to the K I resonance line. First, an empirical measurement of any asymmetry in the line is made by measuring its line bisector and comparing it with those of other metal-poor dwarf and subgiant stars. This is then followed by spectrum synthesis of the line in order to set quantitative limits on any underlying asymmetries that would also affect the Li I feature.

3.1. *The Line Bisector of the* K I *Line*

A simple method to investigate convective motions, which manifest themselves as line asymmetries, is the line bisector technique pioneered by Gray (1980, 1982). Line asymmetries are caused by the combination of blueshifted, hot, rising gas and redshifted, cooler, falling gas in a star's convective atmosphere. Line bisectors are defined by the midpoints of horizontal line segments bounded by the line profile. Because different flux levels in a line profile are emitted from different layers in the atmosphere, the shape of the bisector provides information on convective motions at that atmospheric level. Different types of stars produce certain bisector shapes, with a sample of typical shapes shown by Gray & Toner (1986). Bisector shapes have been studied recently in two metal-poor halo stars, including HD 140283, a subgiant not too dissimilar to HD 84937 (Allende Prieto et al. 1999).

The shape of the line bisector for the K I 7698.97 Å line in HD 84937 is shown in Figure 2. The solid curve illustrates the general trend of the bisectors with line depth and is not any sort of fit. The somewhat C-shaped form of the bisectors is typical of dwarf and subgiant stars with temperatures not too different from that of the Sun. The total velocity spread in the bisectors (~ 0.5 km s^{-1}) is also quite typical for dwarf and subgiant stars (Gray & Toner 1986). It is to be noted that the velocity spread is about one-third the isotopic lithium wavelength shift. The K I bisector is similar to that reported by Allende Prieto et al. (1999) for excited and stronger lines of (mostly) Fe I in the halo stars HD 140283 and Groombridge 1830. The much weaker K I line analyzed in HD 84937 shows a more pronounced reversal of the bisector—about 400 m s^{-1}, compared with about 300 m s^{-1} for the stronger Fe I lines in HD 140283 and only about

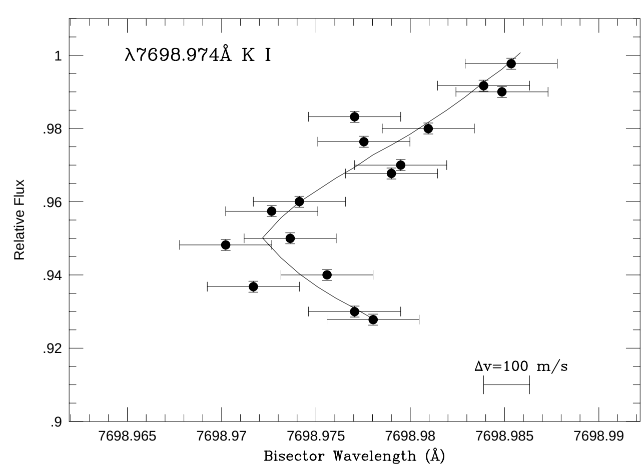

FIG. 2.—Line bisectors for the K I line in HD 84937 as measured from the spectrum shown in Fig. 1. The solid curve is not a fit but is simply drawn through the approximate averages of the points. There is a clear C-shaped pattern in the bisectors.

20 m s^{-1} for Gmb 1830. In comparing these bisector amplitudes it is perhaps worth noting that both HD 84937 and HD 140283 have evolved slightly past the main-sequence turnoff, while Gmb 1830 is still on the main sequence. This similarity suggests that earlier use of excited Ca I lines to constrain the contribution of convective motions to the Li I line's asymmetry did not introduce a significant systematic error in the determination of the fractional ^{6}Li abundance. More quantitative limits on the effects of the line asymmetry can be derived from syntheses of the K I line profile.

3.2. *Spectrum Synthesis of the* K I *Line Profile*

In order to synthesize the K I line profile in HD 84937, the stellar parameters were taken from Smith et al. (1998): $T_{\rm eff} = 6310$ K, $\log g = 4.10$, [Fe/H] $= -2.2$, and a microturbulent velocity $\xi = 1.5$ km s^{-1}. With an equivalent width of 16.4 ± 0.2 mÅ and a MARCS model atmosphere, the K LTE abundance in HD 84937 is $\log \epsilon({\rm K}) = \log [N({\rm K})/N({\rm H})] + 12.0 = 3.41$, or $[{\rm K/H}] = -1.72$; this abundance is derived adopting the accurate *gf*-value of 0.676 (Reader et al. 1980). Adopting $[{\rm Fe/H}] = -2.20$, we have $[{\rm K/Fe}] = 0.48$. A slight overabundance of K relative to Fe has been found from earlier LTE abundance analyses using the K I resonance lines (Gratton & Sneden 1987; Chen et al. 2000). According to non-LTE calculations by Ivanova & Shimansky (2000), the non-LTE K abundance is lower by about 0.16 dex. Thévenin & Idiart (1999), who report on non-LTE calculations for iron, obtain a non-LTE Fe abundance of $[{\rm Fe/H}] = -1.86$ for a model atmosphere and a set of iron lines that gave an LTE abundance of $[{\rm Fe/H}] = -2.10$. If we adopt the non-LTE corrections for K and Fe (assuming an LTE abundance of $[{\rm Fe/H}] = -2.2$), the abundance ratio is $[{\rm K/Fe}] = 0.08$, with the largest uncertainty likely coming from the non-LTE calculations. Line profiles computed under the assumptions of LTE and non-LTE will differ slightly. We ignore this difference.

The line list used to synthesize the K I region was constructed from the Kurucz & Bell (1995) database, and the LTE synthesis code employed was an updated version of MOOG, first developed by Sneden (1973). The K I λ7699 appears unblended. Although quite negligible, the hyperfine and isotopic splitting of the two stable isotopes ^{39}K and ^{41}K was included, with the isotopic ratio set at the terrestrial ratio of $^{39}{\rm K}:^{41}{\rm K} = 93:7$.

Given the stellar parameters and model atmosphere, MOOG implicitly calculates the thermal and van der Waals broadening, with the instrumental profile included as a Gaussian broadening term. A comparison with the observed spectrum of HD 84937 then reveals, as is true for all dwarf/subgiant stars with near-solar temperatures, that the observed line width is broader than the computed line width. The extra broadening is some combination of stellar rotation ($v \sin i$) and macroturbulence (Γ). In the case of HD 84937, experiments with combinations of $v \sin i$ and Γ reveal no evidence of detectable stellar rotation down to values of ~ 2 km s^{-1}; including projected rotational velocities larger than this degrades the comparison between observed and synthetic spectra. Syntheses were then computed with $v \sin i$ set to 1 km s^{-1}, varying Γ to find the best fit between observed and synthetic spectra. This procedure provides a synthetic profile that is symmetric, i.e., no attempt is made to reproduce the slight asymmetry revealed by the C-shaped line bisector. We mention that R. Peterson (2000, private communication) indicated that she has detected a projected rotational velocity in HD 84937 of ~ 3 km s^{-1}. Given the uncertainties in fitting rotational and macroturbulent profiles from the few lines studied to date in HD 84937, our upper limit of 2 km s^{-1} is not in disagreement with 3 km s^{-1}, and using $v \sin i = 3$ km s^{-1} (with an appropriate adjustment in Γ) in HD 84937 would not significantly alter the spectral fits. Observers should note that even higher S/N spectra at $R \geq 120{,}000$ of HD 84937 would be most useful for disentangling and accurately defining rotation and macroturbulence in this star.

The quality of the fits between observed and synthetic spectra is shown in Figure 3, where the values of reduced χ^2 (χ_r^2) are shown versus macroturbulent velocity (Γ). The χ_r^2 is calculated from

$$\chi_r^2 = \frac{1}{\nu - 1} \sum_i \frac{(O_i - S_i)^2}{\sigma_i^2}\,, \tag{1}$$

where ν is the number of degrees of freedom in the fit, O and S are the observed and synthetic spectral points, respectively, and σ is the standard deviation in the observed spectral points. In determining the best values of χ_r^2, a shift in wavelength of the observed spectrum must be applied (the radial velocity), as well as a continuum level shift, along with the input potassium abundance and stellar broadening. The spectral points included in the fit of the line profile spanned ~ 0.6 Å, centered on the K I line center: this amounted to 43 pixels. The total degrees of freedom were thus 43 plus four fitting parameters, or 47. In practice, the wavelength shift was allowed to vary from fit to fit by 5 mÅ and the continuum level shift by 0.002. These small shifts have no significant effect on the overall quality of the fits and their relative values. The potassium abundance can also be allowed to vary slightly; however, this produces no effect on the quality of the fits affected by isotopic or asymmetric convective broadening. As discussed below, the underlying stellar broadening, characterized by the macroturbulence, is also allowed to vary from fit to fit. Values of $\chi_r^2 \sim 1$ indicate good fits of synthetic spectra (models) to the observed spectrum (data). Noting first the curve labeled "No Extra Component," it is clear that the best fit to the observed spectrum of HD 84937 is for a macroturbulent velocity $\Gamma = 5.7$ km s^{-1}. This is in excellent agreement with the value of 6.0 km s^{-1} derived by Smith et al. (1998) using the Ca I 6162 Å line. This is the result derived when no artificial components are added to the K I line, and the best-fit value of χ_r^2 for the line profile is in agreement with the same fits to equal wavelength intervals of continua on both blue and red sides of the K I line. The continuum regions are shown by the nearly horizontal dash-dotted lines, and each separate continuum fit follows from the different sets of K I components described below (but none of the continuum fits are significantly different, as can be seen from Fig. 3).

The additional component fits in Figure 3, labeled 3%, 5%, and 7%, correspond to the addition of a K I component redshifted by the same amount as ^{6}Li is from ^{7}Li (6.9 km s^{-1}) and to the fractional amount of total potassium indicated by the percentages. Here the fits are obviously degraded from the single-component model, even allowing for different values of Γ, small shifts in continuum placement (which cause the small differences in the continuum fits), and wavelength shifts in an effort to obtain the minimum value of χ_r^2. Addition of a redshifted component degrades the fit to the observed line. This is a strong indication that the reported detections of ^{6}Li in HD 84937 are real.

Direct comparisons of synthetic and the observed spectra are illustrated in Figure 4. The top panel shows the observed spectrum (*circles*) with the various synthetic spectra shown as solid curves; the curves with increasing contributions from red wings are the extra K I components (3%, 5%, and 7%). The bottom panel shows the residuals (observed minus synthetic). The single component can be seen to provide the best overall fit, with the red wings produced by redshifted components not in evidence in the observed spectrum.

Figure 5 quantifies the significance of the comparison between observed and synthetic spectra by plotting χ_r^2 versus fraction of a redshifted component. One-, two-, and three-sigma limits to the fits are shown as dashed lines,

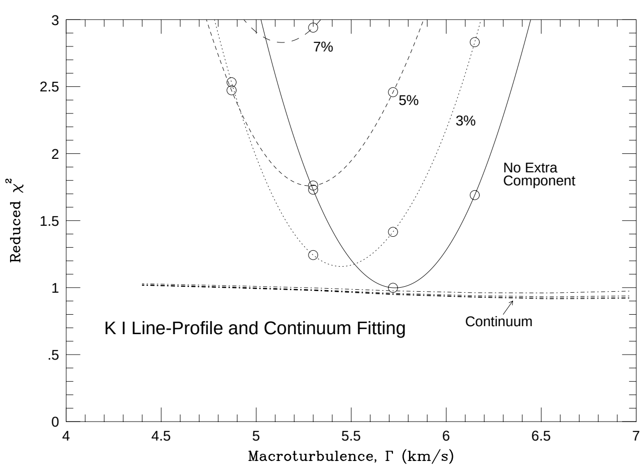

FIG. 3.—Reduced χ^2 fits of synthetic spectra to the observed K I line in HD 84937 for different assumed structures of K I (single or added redshifted components containing various amounts of fractional absorption), as a function of the macroturbulent velocity. Redshifted components have been shifted by the amount that ^{6}Li is isotopically shifted from ^{7}Li. The single-component K I profile provides the best fit to the observed spectrum.

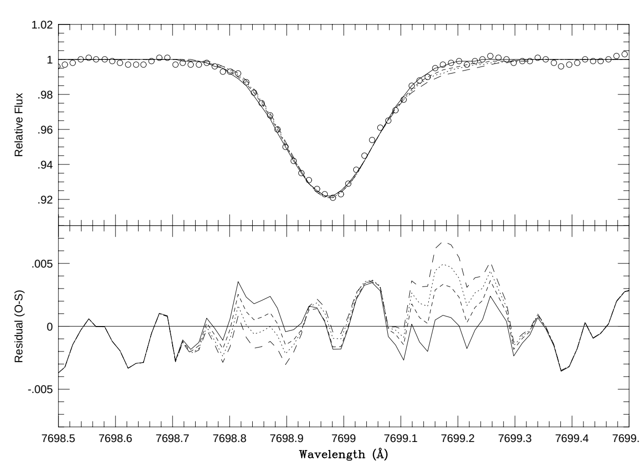

FIG. 4.—*Top*: Synthetic fits to the K I line profile in HD 84937, along with the observed spectrum (*circles*). The different synthetic profiles with small red wings correspond to extra fractional absorption components of 3%, 5%, and 7%. *Bottom*: Residuals (observed minus synthesis), with the synthetic line profile with no extra component providing the minimum in the residuals.

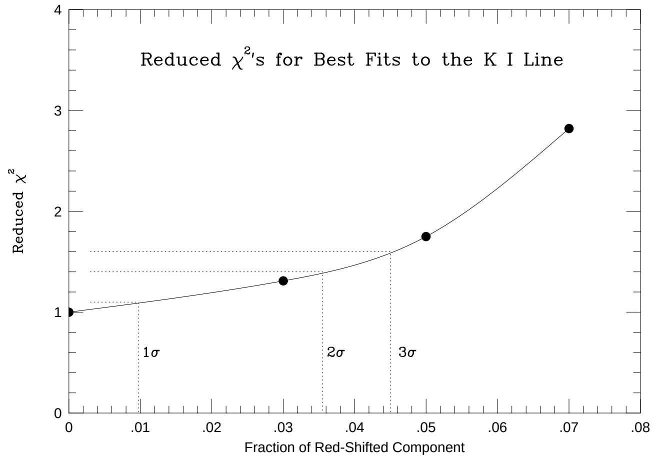

FIG. 5.—Reduced χ^2 as a function of fraction of redshifted absorption. The best fit is for the single component, with χ_r^2 increasing with fraction of redshifted component. The 1 σ, 2 σ, and 3 σ confidence limits are also indicated.

based on the standard statistical tables from Bevington (1969). At approximately the 2 σ level, redshifted components greater than about 0.035 fraction of total K I absorption can be ruled out. As summarized by Cayrel et al. (1999), the best estimate of $f(^6\text{Li})$ in HD 84937 is 0.052 ± 0.019. Based on the analysis of the K I profile presented here, it is increasingly unlikely that the detected ^{6}Li in HD 84937 could be caused entirely by a redshifted ^{7}Li component.

4. DISCUSSION AND CONCLUSIONS

The K I line profile in HD 84937, as modeled using a high-S/N (~ 550), high-resolution ($R = 110{,}000$) spectrum, has been found to be single to high accuracy; any redshifted component is ≤ 0.01 fractional absorption at the 1 σ level. Because the Li I and K I lines are formed at nearly identical levels in the atmosphere of HD 84937, this result suggests strongly that the Li I line profile is not affected significantly by any redshifted components of such a nature as to be confused with ^{6}Li.

In our discussion, we assume that the slight asymmetry of the K I 7699 Å line is caused by convective motions, but no attempt is made to model this asymmetry. Nissen et al. (2000), in their analysis of a similar turnoff star, show that line profiles computed using three-dimensional hydrodynamic model atmospheres provide an excellent fit to the observed profiles of the Ca I, Fe I, and K I 7699 Å lines. Yet, the same ^{6}Li fractional abundance is obtained with the classical one-dimensional models as with the three-dimensional models. This suggests that our empirical approach suffices to eliminate the possibility that the ^{6}Li detections reflected an unacknowledged contribution of atmospheric motions to the Li I line profile.

Because of the importance of reported ^{6}Li detections in halo stars to our understanding of big bang nucleosynthesis and light-element synthesis in the intergalactic medium and the early Galaxy, it was important to demonstrate that the ^{6}Li signal, a slight additional asymmetry to the Li I 6707 Å line, was not a signature of convective motions in the stellar atmosphere. Our study shows that the reported detections of ^{6}Li in HD 84937 (Smith et al. 1993, 1998; Hobbs & Thorburn 1994, 1997; Cayrel et al. 1999) are most probably real.

It is a pleasure to thank the staff of McDonald Observatory for maintaining excellent spectroscopic facilities. Partial support (V. V. S.) was provided by the Texas Advanced Research Program (003661-0003-1999), NASA's Long Term Space Astrophysics Program (NAG 5-9213), and the National Science Foundation (AST 96-18459). D. L. L. acknowledges support from the National Science Foundation (AST 96-18414) and the Robert A. Welch Foundation of Houston, Texas.

REFERENCES

Allende Prieto, C., García López, R. J., Lambert, D. L., & Gustafsson, B. 1999, ApJ, 526, 991

Bevington, P. R. 1969, Data Reduction and Error Analysis for the Physical Sciences (New York: McGraw-Hill)

Cayrel, R., Spite, M., Spite, F., Vangioni-Flan, E., Cassé, M., & Audouze, J. 1999, A&A, 343, 923

Cecil, F. E., Yan, J., & Galovich, C. S. 1996, Phys. Rev. C, 53, 1967

Chen, Y. Q., Nissen, P. E., Zhao. G., Zhang, H. W., & Benoni, T. 2000, A&AS, 141, 491

Gratton, R. G., & Sneden, C. 1987, A&A, 178, 179

Gray, D. F. 1980, ApJ, 235, 508

———. 1982, ApJ, 255, 200

Gray, D. F., & Toner, C. G. 1986, PASP, 98, 499

Hobbs, L. M., & Thorburn, J. A. 1994, ApJ, 428, L25

———. 1997, ApJ, 491, 772

Ivanova, D. V., & Shimansky, V. V. 2000, AZh, 77, 432 (English transl. Astron. Rep., 44, 376)

Kurucz, R. L., & Bell, B. 1995, CD-ROM 23, Atomic Line Data (Cambridge: Smithsonian Astrophys. Obs.)

Nissen, P. E., Asplund, M., Hill, V., & D'Odorico, S. 2000, A&A, 357, L49

Nissen, P. E., Lambert, D. L., Primas, F., & Smith, V. V. 1999, A&A, 348, 211

Reader, J., Corliss, C. H., Wiese W. L., & Martin, G. A. 1980, Wavelengths and Transition Probabilities for Atoms and Atomic Ions (Natl. Stand. Ref. Data Ser. 68) (Washington: Natl. Bur. Stand.)

Smith, V. V., Lambert, D. L., & Nissen, P. E. 1993, ApJ, 408, 262

———. 1998, ApJ, 506, 405

Sneden, C. 1973, Ph.D. thesis, Univ. Texas

Thévenin, F., & Idiart, T. P. 1999, ApJ, 521, 753

Tull, R. G., MacQueen, P. J., Sneden, C., & Lambert, D. L., 1995, PASP, 107, 251

Vangioni-Flam, E., Coc, A., & Cassé, M. 2000, A&A, 360, 15